Theoretical Chemistry Accounts (2019) 138:16
https://doi.org/10.1007/s00214-018-2405-y

REGULAR ARTICLE

Effects of substitutional Mo and Cr on site occupation and diffusion of hydrogen in the β-phase vanadium hydride by first principles calculations

Thi Viet Bac Phung[1] · Hiroshi Ogawa[2] · Van An Dinh[1,3] · Oanh Hoang Nguyen[1,4] · Yoji Shibutani[1,3] · Kohta Asano[2] · Yumiko Nakamura[2] · Etsuo Akiba[5]

Received: 18 May 2018 / Accepted: 17 December 2018 / Published online: 3 January 2019

Abstract

The effects of substitutional Mo and Cr in β-phase $VH_{0.5}$ and $V_{1-x}M_xH_{0.5625}$ (M = Mo, Cr; x = 0, 0.0625, 0.125) on the site occupation and diffusion paths of hydrogen are investigated by quantum mechanical calculations based on density functional theory. Fundamental processes of the interstitial-assisted mechanisms are systematically figured out, and specific values of the site energies are obtained with zero-point energy (ZPE) corrections. Hydrogen atoms are found to occupy the octahedral (O) interstitial sites in β-phase $(V+M)H_{0.5}$ in the ground state. Upon increasing the hydrogen concentration H/(V + M) higher than 0.5, the additional H atom prefers to reside at the tetrahedral (T) interstitial sites. The minimum energy paths of hydrogen diffusion are analyzed by the Nudged Elastic Band method with ZPE corrections. The site occupation energy and activation energy for each hydrogen diffusion path are found to be strongly influenced by the substitution of Mo or Cr into vanadium hydride. The results presented in this work indicate that the additional H prefers to migrate directly from T site to the nearest neighboring T site without crossing O site. The energy barriers in the order of 0.253–0.276 eV of hydrogen migration in the $V_{1-x}M_xH_{0.5625}$ hydrides obtained from ab initio simulations are in good agreement with the experimental data by means of ^{1}H NMR measurement.

Keywords Hydrogen storage vanadium hydrides · Mo/Cr substitution · Hydrogen diffusion · DFT calculations

1 Introduction

It is considered that hydrogen is going to fuel the next generation vehicles. Hydrogen is the most abundant element on earth and is regenerative and environmentally friendly. Hydrogen fuel provided by green method is renewable [1–3]. Hydrogen burns cleanly in air, the only product is water. The development of viable hydrogen storage system is becoming increasingly important for promoting the hydrogen economy. Various hydrogen storage materials, such as metal hydrides, carbon-based materials, and complex metal hydrides have been investigated [4]. The highest volumetric densities of hydrogen are found in metal hydrides. Many metals and alloys are capable of reversibly absorbing large amounts of hydrogen. Metal hydrides compose of metal atoms that constitute a host lattice and hydrogen atoms. The elements of group V, such as vanadium, can combine with hydrogen in interstitials up to the hydrogen-to-metal atomic ratio H/M ≈ 2 to form a large variety of metal–hydrogen complexes [5].

Electronic supplementary material The online version of this article (https://doi.org/10.1007/s00214-018-2405-y) contains supplementary material, which is available to authorized users.

✉ Thi Viet Bac Phung
phungthivietbac@vnu.edu.vn; ptv.bac@vju.ac.vn

[1] Nanotechnology Program, VNU Vietnam Japan University, My Dinh Campus, Nam Tu Liem, Hanoi, Vietnam

[2] National Institute of Advanced Industrial Science and Technology, AIST Tsukuba Central 5, 1-1-1 Higashi, Tsukuba 305-8565, Japan

[3] Center for Atomic and Molecular Technologies, Graduate School of Engineering, Osaka University, Yamadaoka 2-1, Suita, Osaka 565-0871, Japan

[4] VNU University of Science, 334 Nguyen Trai, Thanh Xuan, Hanoi, Vietnam

[5] Department of Mechanical Engineering, Faculty of Engineering, Kyushu University, 744 Motooka, Nishi-ku, Fukuoka 819-0395, Japan

Vanadium is a transition metal with the electronic configuration $[Ar]3d^3 4s^2$. The XRD measurements showed that vanadium forms the hydrogen solid solution phase with a BCC structure (α phase), the monohydride phase V_2H with a body-centered tetragonal (BCT) structure (β phase), and the dihydride phase VH_2 with a face-centered cubic (FCC) structure (γ phase) at ambient temperatures [6, 7].

$$V_2H(\beta) + \frac{3}{2}H_2 \leftrightarrow 2VH_2(\gamma) \quad (1)$$

In the α phase and the β phase, only some hydrogen atoms are absorbed and in γ phase the hydride is fully formed. Vanadium-based BCC alloys containing Mo, Cr, and other transition metals have been known to improve hydrogen storage properties [8–10]. Hydrogen dynamics in metal and alloying powders [11–14] can be measured by nuclear magnetic resonance (NMR) spectroscopy; however, the mechanism of the hydrogen diffusion is not revealed. Mo and Cr addition possibly affects not only diffusion but also site occupation of hydrogen in the metal lattice because it causes the lowered stability of the hydride phase [15]. The site occupation of hydrogen in the β phase has been discussed by analyzing the temperature dependence of the spin–lattice relaxation time.

It is known that in the β-phase vanadium hydrides, hydrogen atoms occupy the octahedral sites between vanadium atoms along the z-axis. Hydrogen atoms in vanadium hydrides are located at a specific octahedral site called O_Z, which is the center of an interstitial octahedron with a fourfold axis toward z. In our present studies, the O_Z sites are divided into two types of interstitial positions O_{Z1} and O_{Z2} as in elongated and compressed octahedrons toward z, respectively. H atoms in vanadium hydrides are preferentially located at the O_{Z1} sites. At condensed hydrogen content, on the other hand, H atoms are predicted to occupy both the O_{Z1} and O_{Z2} sites randomly because the interstitial octahedron volume is larger than the tetrahedron one. However, in the previous experimental study by means of NMR [15, 16], the T-site occupation of hydrogen was observed. Experimentally, this phenomenon is not well understood. The influence of lattice uniaxial strain on the site occupancy of hydrogen in vanadium, particularly on the preferred octahedral occupancy of hydrogen in strained vanadium layers, has been studied recently by the density functional theory [17]. At different hydrogen concentrations, the switch from T- to O-site occupancy or the reverse switch from O to T has been found to be dependent on the uniaxial lattice expansion quantified by the c/a ratio.

Although the electronic states of vanadium hydride have been studied extensively [18–22], the hydrogen behaviors in this metal hydride have not been well characterized. Therefore, it is needed to investigate systematically the behavior of hydrogen (particularly, the site occupation and diffusion of hydrogen) in metal hydrides and the different alloying systems by computational methods. In this study, we investigate the migration of hydrogen in monohydride vanadium hydride and alloys using the density functional theory (DFT) method. The preferable site occupation at H content higher than $H/(V+M) = 0.5$ (the hydrogen-to-metal atomic ratio) is precisely determined. The atomistic behavior of hydrogen in β-phase $V_{1-x}M_xH_{0.5625}$ hydrides is investigated to explore the influence of substitutional Mo and Cr on the site occupation and diffusion paths of hydrogen. The energy barriers of hydrogen diffusion for the T and O sites are estimated and compared to the previous ^{1}H MNR measurement [15, 16]. The mechanism of hydrogen diffusion in the β-phase vanadium hydrides with Cr and Mo addition is discussed. Most importantly, energetic characteristics such as the site occupation energy and activation energy for each diffusion path, which have not been experimentally determined, are evaluated from our current theoretical calculations.

1.1 Theoretical method and computational details

We performed density functional theory (DFT) [23, 24] calculations within the generalized gradient approximation (GGA) of the GGA-PBE form for electron exchange and correlation, using the Vienna Ab initio Simulation Package (VASP) [25, 26]. Here we employed Blochl's projector augmented wave (PAW) method, as implemented by Kresse and Joubert. The PAW method is an all-electron DFT technique (within the frozen-core approximation) with the computational efficiency of pseudopotential techniques [27–29]. We tested k-point sampling and kinetic energy cutoff convergence for all super cells with Monkhorst–Pack [30, 31] k-point meshes to indicate that total energies for all cells are converged. The converged plane wave cutoff energy of 450 eV was taken for all calculations. Structural relaxations were performed using $8\times8\times8$ gamma-centered k-point grid. To find the ground state structure of β-$VH_{0.5}$ (the monohydride phase V_2H), both the cell shape and atomic positions in super cells are allowed to relax.

The computational models of β-$VH_{0.5}$ were based on a $2\times2\times2$ body-centered metal cell. The structure configurations are composed of $V_{16}H_8$, $V_{16}H_9$, $V_{15}MoH_8$, $V_{15}CrH_8$, $V_{14}Mo_2H_8$, $V_{14}Cr_2H_8$, $V_{15}MoH_9$, $V_{15}CrH_9$, $V_{14}Mo_2H_9$, and $V_{14}Cr_2H_9$. The full optimization is performed in calculating the equilibrium lattice constants for the bulk crystal and for the metal hydrides with the hydrogen atoms placed at the specific interstitial locations. The zero-point energy (ZPE) corrections (which are calculated from the harmonic approximation of the potential energy change as a function of atomic displacement of hydrogen atom) are also added into the total energy in order to determine precisely the energy barrier for hydrogen diffusion.

The minimum energy paths (MEPs) of hydrogen diffusion were analyzed by the Nudged Elastic Band (NEB) method [32]. In NEB method, the constrained optimization is done by adding spring forces along the band between images and by projecting out the component of the force due to the potential perpendicular to the band. All the discrete configurations between two interstitial sites were optimized simultaneously along the hydrogen diffusion path until the maximum residual forces acting on the atoms reached below 0.001 eV/Å. The initial images of diffusing H atom are assumed to be on the lines connecting neighboring interstitial sites of the BCT structure illustrated in Fig. 1. Diffusion path is considered as a set of elementary diffusion processes (EDP). Barrier of hydrogen diffusion is estimated from the activation energy of EDPs along the certain path. To characterize the nature of the hydrogen transfer in the metal hydride, the atomic charge of the hydrogen along the diffusion path is calculated using a Bader charge analysis [33–35].

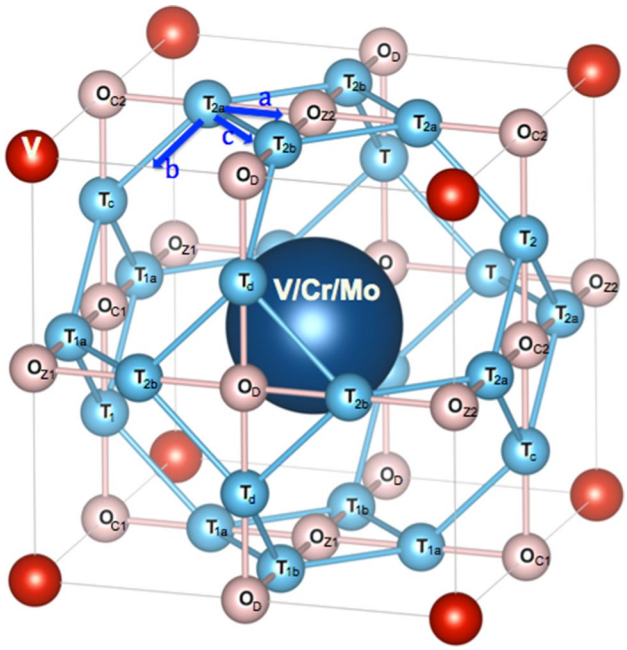

Fig. 1 Schematic diagram of the interstitial *T*- and *O*-sites positions in β-$VH_{0.5}$ with notation Wyckoff positions of *T* and *O* sites in BCT structure. O_{Z1}-site hydrogen atoms are occupied in β-$VH_{0.5}$ and alloying hydrides. *T* sites and *O* sites are denoted by light blue and light pink balls, respectively. Vanadium atoms are shown by red balls; substituted Mo/Cr atoms are displayed by large blue balls in the center of unit cell. The arrows *a, b, c* starting from T_{2a} site show the diffusion path directions of H atom which is assumed Fig. 4a–c

2 Results and discussion

2.1 Lattice parameters

Firstly, the structures of β-$VH_{0.5}$ proposed by Noda [36] are determined by full relaxation of tetragonal (space group $I4_1/amd$) and monoclinic (space group *Cm*) structures. Both structures can be synthesized depending on the tensile stress applied during crystal growth. In both the monoclinic and tetragonal structures, H atoms are preferentially located at the O_{Z1} sites. The calculated results for the structure stability show that the tetragonal structure is more stable by 0.02 eV compared to monoclinic structure. Thus, hereafter the tetragonal structure is adopted in our study. The optimized super cell is described as parameters $a \approx 2a_0 = 5.747$ Å and $c \approx 2c_0 = 6.713$ Å, where a_0 and c_0 are unit cell dimensions of the body-centered conventional cell. The calculated lattice constants at 0 K differ by 4.23% from the experimental values at room temperature [37]. Calculated Wyckoff positions of vanadium in three monohydrides are given in Table 1. The displacements of vanadium atoms from $z = 0.25$ to $z \approx 0.27$ are caused by H atoms at the O_{Z1}-site occupancy. In other words, H atoms at O_{Z1} site occupy the elongated large octahedral interstices toward *z*. These structures are in good agreement with the experimental observation.

The influence of Mo or Cr substitution on the volume, lattice parameters *a* and *c*, and *c*/*a* ratio of $V_{1-x}M_xH_{0.5}$ ($x = 0.0625$, 0.125) are shown in Fig. 2a–c. The volume is expanded by addition of Mo, but that is compressed by addition of Cr. It is caused by the difference in atomic radii of V, Mo, and Cr, which are 1.32, 1.36, and 1.25 Å, respectively. The alloying Mo/V and Cr/V monohydrides also have BCT structures as pure vanadium hydride $VH_{0.5}$. Calculated and experimental volumes show a similar variation as can be seen in Fig. 2a. While the lattice parameter *c* decreases for both Mo and Cr cases, the lattice parameter *a*, on the other hand, increases in the case of Mo but decreases in the Cr case, as shown in Fig. 2b. As a result, the *c*/*a* ratio decreases

Table 1 Atomic parameters for metal atoms in three monohydrides $V_{16}H_8$, $V_{15}MoH_8$, and $V_{15}MoH_8$

Metal atoms	Wyckoff index	Coordinates		
		x	*y*	*z*
V in $V_{16}H_8$	16h	0.0000	0.5001	0.2696
V/Mo in $V_{15}MoH_8$ (averaged)	16h	0.0000	0.5003	0.2682
V/Cr in $V_{15}CrH_8$ (averaged)	16h	0.0000	0.5000	0.2502

Coordinates of metallic atoms in $V_{15}MoH_8$ and $V_{15}CrH_8$ are the averaged values with assuming $I4_1/amd$ symmetry space group

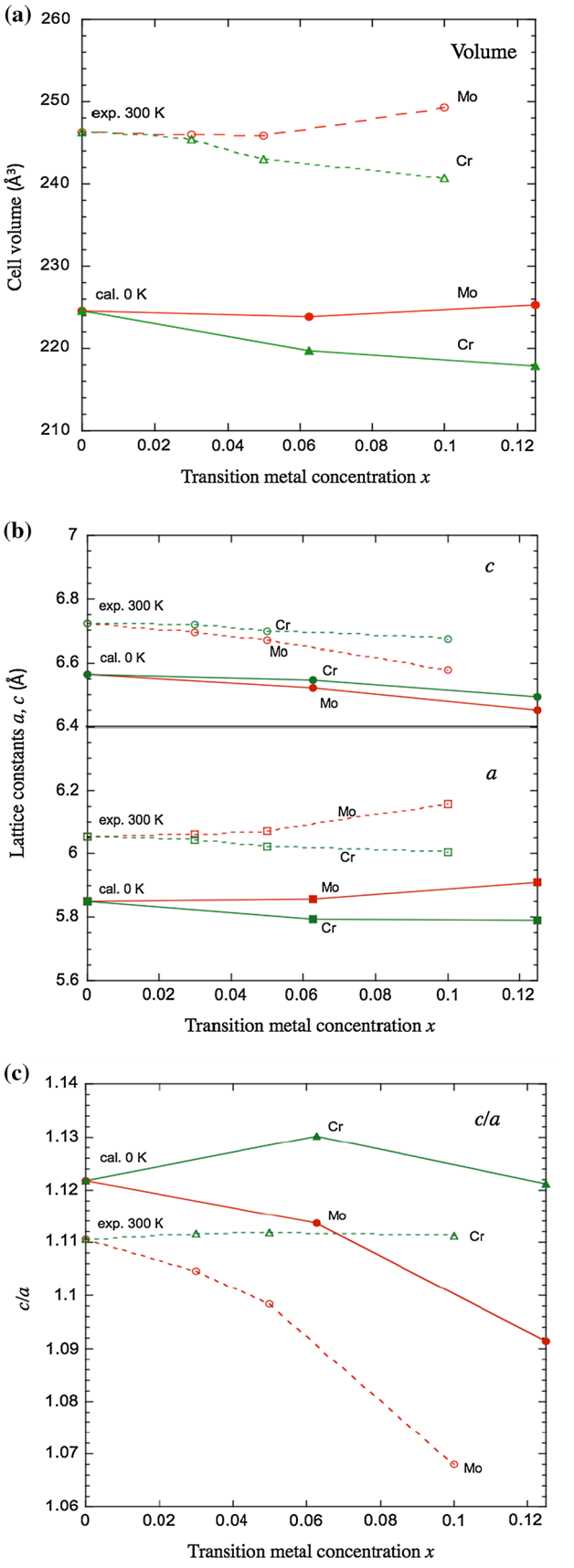

Fig. 2 The influence of Mo or Cr substitution on the volume, lattice parameters a and c, and c/a ratio of $V_{1-x}M_xH_{0.5}$ ($x=0.0625$, 0.125). **a** Optimized super cell volume of $V_{1-x}M_xH_{0.5}$ ($x=0.0625$, 0.125) at 0 K (displayed by the solid lines) compared with the experimental data by ^{1}H NMR[15, 16] for $V_{1-x}M_xH_{0.68}$ (displayed by the dashed lines). **b** Optimized lattice parameters c and a of $V_{1-x}Mo_xH_{0.5}$ ($x=0.0625$, 0.125) at 0 K (displayed by the solid lines) compared with the experimental data by ^{1}H NMR[15, 16] for $V_{1-x}M_xH_{0.68}$ (displayed by the dashed lines). The upper part is lattice constant c and the lower part is lattice constant a. **c**. The c/a ratio of $V_{1-x}Cr_xH_{0.5}$ ($x=0.0625$, 0.125) at 0 K (displayed by the solid lines) compared with the experimental data by ^{1}H NMR[15, 16] for $V_{1-x}M_xH_{0.68}$ (displayed by the dashed lines)

with increasing Mo content, while this ratio does not change significantly in the case of Cr (see Fig. 2c). This behavior agrees well with the observation in our previous studies by ^{1}H NMR measurement. It was suggested that O_{Z1} hydrogen atom in the BCT structure is most stable at $c/a \approx 1.1$. The present result implies that the addition of Mo and Cr changes the interaction between hydrogen and metal atoms, changes the shapes of interstices, and hence leads to change the site occupation of additional hydrogen into the monohydride phase. Therefore, the preferred site occupancy of hydrogen is determined by the lattice expansion.

2.2 The site occupancy

We examine the site occupancy of H atom at the possible sites where H prefers to occupy at hydrogen concentration higher than H/(V + M) = 0.5. This investigation is essential in order to confirm the results from ^{1}H NMR measurement. Hence, we analyze the β-phase structures including one additional H atom to have similar H content in the metal hydrides. The site energy for the additional H atom, E_{site}, is evaluated by

$$E_{\text{site}} = E_{V_{16-n}M_nH_9} - \left(E_{V_{16-n}M_nH_8} + \frac{1}{2}E_{H_2}\right); \quad n = 0, 1$$

where $V_{16-n}M_nH_9$ is composed of β-phase $V_{16-n}M_nH_8$ with one H atom at any T or O site given in Fig. 1. The subscripts indicate the Wyckoff notation and different symmetry positions of interstitial sites, i.e., O_{z1}, T_2, T_c.

The formation energy of hydrogen molecule in gas phase E_{H2} is calculated for a H_2 molecule in a cubic cell with size of 15 × 15 × 15 Å^3. It should be noted that ½ E_{H2} is the energy per one atom of H in the hydrogen molecule. The dissociation energy of hydrogen molecule is calculated to be 4.52 eV and in a good agreement with experimental data[5] of 4.48 eV. The H sites given in Fig. 1 should split into several asymmetric sites by Mo/Cr substitution. In fact, they show small splitting of energy level for the same type of H site because the substitutions of Mo/Cr distort the interstitial sites and change the equilibrium position of additional H atom. In order to see the influence of Mo/Cr substitution, we add a H atom into a few asymmetric positions for each

interstitial in the vicinity of the substituted metal atom and calculated the site energy.

The calculated site energies for pure and substituted cases are acquired and summarized in Table 2. For some *O*-site positions, the E_H values of H-site energy are not available due to the shift of additional H atoms from these *O*-site positions to the nearest neighbor *T* site. The site energy with ZPE correction is presented in the parentheses; the incorporation of ZPE corrections has a significant effect on the site energy. The ZPE corrections depend on the specific hydrogen site; the equivalent ZPE of 1/2 hν is on the order of 0.001–0.002 eV when changing the additional hydrogen position. These corrections do not alter the tendency with regards to the most stable site occupation. The result shows that the *T* sites near the occupied O_{Z1} site (1*a* and 1*b*) and the unoccupied *O* sites (*C*1, *C*2, and *D*) are comparatively unstable. On the other hand, *T* sites far from the O_{Z1} sites (2*a*, 2*b*) are more stable. The result indicates that H atoms partly occupy *T* sites at higher H-content region $H > 0.5(V + M)$.

The number of H atoms at *T* site in pure and substituted structures is estimated by changing the initial position of the additional H atom. It is found that some of the hydrogen atoms at O_{Z1} site and O_{C1} site are switched to the neighboring *T* sites (1*a* or 1*b*) by the lattice deformation due to the additional H atom. This caused by two possible driving forces: substitution of transition metals Mo/Cr and addition of excess H atom into β-V_2H. This effect is significant in the substitutional Mo case and less significant in the substitutional Cr one. This finding is consistent with our studies by means of the ^{1}H NMR observation on $V_{1-x}M_xH_{0.68}$ [15, 16] and by classical molecular dynamics simulation [38].

When hydrogen atoms are introduced into vanadium to form β-phase vanadium hydrides, hydrogen atoms reside in certain octahedral positions. At the higher H content, additional H atom caused the effect of distorted metal lattice in the BCT β-phase hydrides. The repulsive interactions at short metal–metal and hydrogen–hydrogen distances result in the shift of the hydrogen-site occupation. Upon increasing the hydrogen concentration higher than $H/(V + M) = 0.5$, the calculated site energy of *T*-sites hydrogen becomes lower than the *O*-sites hydrogen. Thus, *T* sites become more preferable than *O* sites for additional hydrogen atom. This finding shows interesting behavior of hydrogen, not like the prediction that hydrogen will occupy the O_{Z1} and O_{Z2} sites randomly in metal hydrides.

The charge transfer between H and other atoms can be described by Bader charge analysis, and the charge acquired by hydrogen in each configuration is shown in Table 2 and in the Supplementary Material. As can be seen, additional hydrogen gains electrons independent of its occupancy at the *T* sites or the *O* sites. The strength of the site energy is related to the hydrogen charge where the stability of the site is increased when hydrogen gains more charge, indicating that strong interactions exist between the hydrogen and its surrounding atoms. In addition, the numbers of site occupation is enhanced by substituting Mo/Cr into vanadium hydrides as given in Table 2. These results confirm the site occupancy in the tetrahedral interstitials as observed in ^{1}H NMR experiment.

Table 2 The calculated H-site energy E_H (eV) and Bader charge Q_H (*e*) of additional H atom in the pure and Mo- or Cr-substituted vanadium monohydride

	$V_{16}H_9$		$V_{15}MoH_9$		$V_{15}CrH_9$	
	E_H (eV)	Q_H (*e*)	E_H (eV)	Q_H (*e*)	E_H (eV)	Q_H (*e*)
T-site position (Wyckoff)						
1*a* (16*h*)	−0.0034 (−0.0028)	−0.82	−0.0055 (−0.0042)	−0.92	−0.0042 (−0.0038)	−0.87
1*b* (16*f*)	−0.0028 (−0.0021)	−0.80	−0.0037 (−0.0032)	−0.88	−0.0079 (−0.0068)	−0.96
2 (4*b*)	−0.0043 (−0.0031)	−0.87	−0.0064 (−0.0055)	−0.94	−0.0097 (−0.0088)	−0.98
2*a* (16*h*)	−0.0512 (−0.0488)	−1.03	−0.0425 (−0.0412)	−0.87	−0.0318 (−0.0315)	−1.00
d (16*g*)	−0.0082 (−0.0075)	−0.97	−0.0173 (−0.0158)	−1.00	−0.0039 (−0.0036)	−0.83
2*b* (16*f*)	−0.0507 (−0.0482)	−1.03	−0.0424 (−0.0409)	−1.01	−0.0208 (−0.0189)	−1.01
c (8*e*)	−0.0182 (−0.0163)	−1.01	−0.0422 (−0.0411)	−1.01	−0.0256 (−0.0244)	−1.01
1 (4*a*)	−0.0081 (−0.0068)	−0.97	−0.0194 (−0.0182)	−1.03	−0.0178 (−0.0159)	−1.00
O-site position (Wyckoff)						
*Z*1 (8*d*)	(Shifted to *T*)		−0.0089 (−0.0072)	−0.84	−0.0081 (−0.0074)	−0.83
*C*2 (8*e*)	(Shifted to *T*)		−0.0042 (−0.0031)	−0.82	−0.0023 (−0.0019)	−0.82
*C*1 (8*e*)	(Shifted to *T*)		−0.0036 (−0.0028)	−0.81	−0.0017 (−0.0015)	−0.78
D (8*e*)	(Shifted to *T*)		(Shifted to *T*)		(Shifted to *T*)	

For some *O*-site positions, the E_H values of H-site energy and the Bader charge Q_H are not available due to the switch of additional H atoms from *O* to *T* site. The site energy with ZPE correction is presented in the parentheses

2.3 The hydrogen diffusion path and energy barrier

Hydrogen diffusion is an important step in kinetics of hydrogenation and dehydrogenation in hydrogen storage materials. After additional H atom resides in the interstitial site, the next issue is where this additional H atom will diffuse in the metal lattice. In order to explain the effect of Mo/Cr substitution on hydrogen diffusion and its activation energy, the NEB calculation is carried out for some possible diffusion paths of hydrogen atom in $V_{1-x}M_xH_{0.5625}$ ($x=0, 0.0625$) systems. We assume three different diffusion paths starting from 2*a* where the site energy is lowest in all systems as shown in Table 2. These paths trace the sites around a pure or substituted metallic atom as (a) 2*a*–*Z*2–2*a*–2–*C*2–*c*, (b) 2*a*–*c*–*C*1–1, and (c) 2*a*–2*b*–*d*–2*b*. Directions of these paths are indicated by arrows in Fig. 1. The migration coordinates with hydrogen displacement along the diffusion paths are illustrated in Fig. 3. Only the 1 × 1 × 1 BCT part in tetragonal super cell (2 × 2 × 2 BCT) is shown in Fig. 3 for simplicity. The atomic charge of the hydrogen along the diffusion path is calculated using a Bader charge analysis. The Bader charge Q_H (e) of the transferred H species in the NEB calculations is presented in the Supplementary Material. The calculated potential energy surfaces along three possible pathways are shown in Fig. 4a–c. It is noted that GGA functionals are largely affected by self-interaction error, so that the barriers could be underestimated.

Not only the diffusion barrier of the hydride changes but also the diffusion distance is increased or decreased due to volume expansion or contraction of the unit cell. After NEB calculation, the vibrational analysis is performed to confirm the imaginary frequency mode of the transition state configuration. The activation energies for hydrogen diffusion with the ZPE corrections, E_0, are summarized in Table 3. The contribution of ZPE to the activation energy is considered for each elementary process of hydrogen diffusion. As seen in Fig. 4a, the activation energy of the hydrogen diffusion between two *T* sites (T_{2a}) via O_{Z2} site is determined as 0.227 eV; the activation energy changes to 0.230 eV and 0.139 eV corresponding to substituted Mo and Cr cases, respectively. Higher activation energies of hydrogen diffusion between T_2 and T_c via O_{C2} site are observed as 0.452 eV, 0.658 eV, 0.399 eV for pure, substituted Mo and Cr cases, respectively. Similarly, significantly high barriers are found when hydrogen diffuses from T_c to T_1 via O_{C1} on the pathway (b) where the activation energies were evaluated as 0.837 eV, 0.997 eV, and 0.706 eV, respectively as shown in Fig. 4b. However, the activation energy for hydrogen diffusion between two *T* sites (T_{2a} and T_c) without crossing *O* site is relatively small as 0.192 eV, and this value is not strongly affected by Mo/Cr substitution. These results indicate that the activation energy of hydrogen diffusion toward $\pm z$ via *O* sites (2*a*) increases by Mo and decreases by Cr substitution.

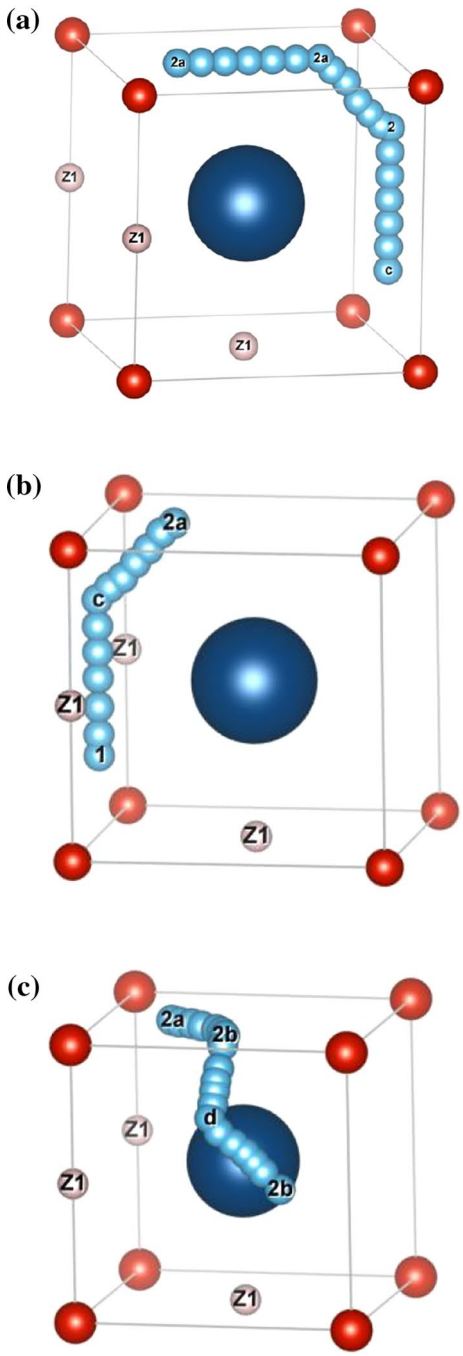

Fig. 3 Modeling of the migration coordinates with hydrogen displacement along three diffusion paths. These paths trace the sites around the pure or substituted metallic atom as **a** 2*a*–*Z*2–2*a*–2–*C*2–*c*, **b** 2*a*–*c*–*C*1–1, and **c** 2*a*–2*b*–*d*–2*b*. Only the 1 × 1 × 1 BCT part in tetragonal super cell (2 × 2 × 2 BCT) is shown for simplicity

Figure 4c shows the profile of activation energy on the pathway (c); in this case, hydrogen diffuses between *T* sites without crossing any *O* site. The activation energy for direct *T*-site–*T*-site diffusion (T_{2b}–T_d) in pure vanadium hydride was determined to be 0.264 eV; this value varies to 0.253 eV

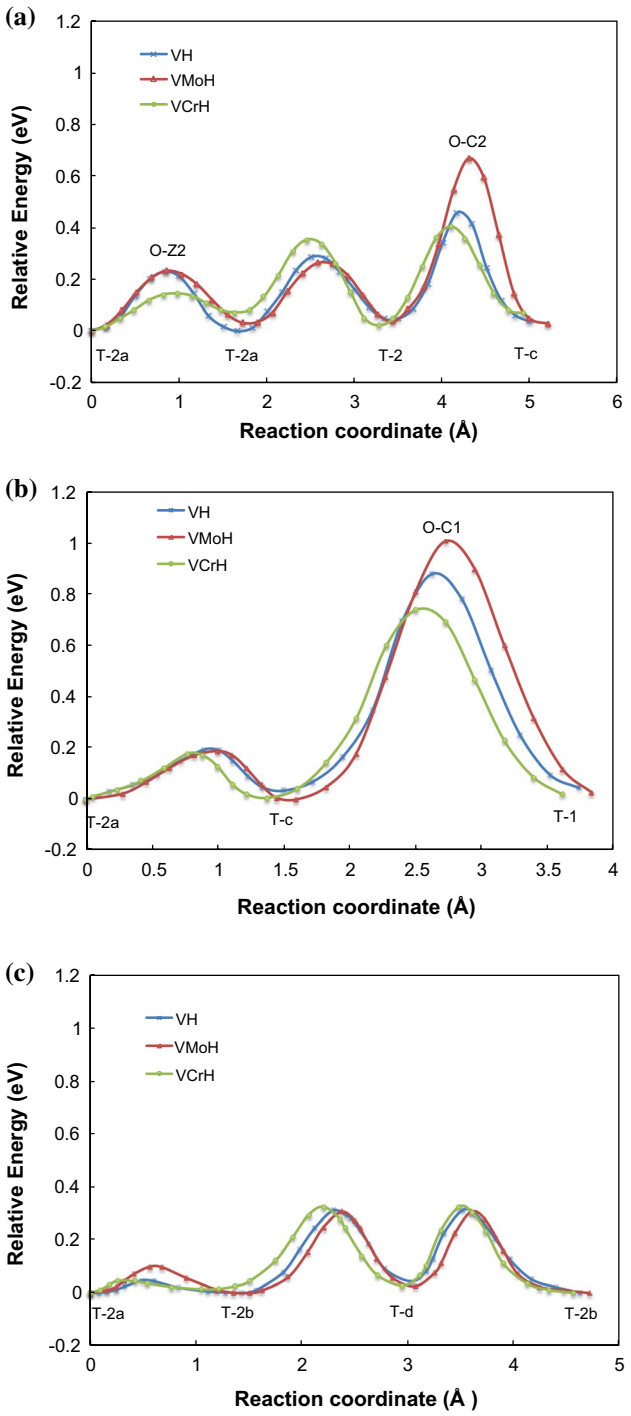

Fig. 4 Potential surfaces of hydrogen diffusion paths starting from the most stable configuration of T_{2a}-site H position according to three pathways are shown in Fig. 1. **a** T_{2a} to a neighboring T_{2a} to T_2 and T_c. **b** T_{2a} to a neighboring T_c to T_1. **c** T_{2a} to T_{2b} to T_d and neighboring T_{2b}

for the case of Mo substitution and to 0.276 eV for the case of Cr substitution as listed in Table 3. The activation energy for hydrogen diffusion from T_{2a} to T_{2b} is relatively small. The barrier of hydrogen diffusion on the pathway (c) is

Table 3 The calculated activation energies ε_a (eV) of elementary diffusion processes (T site–O site–T site and T site–T site) along the diffusion paths in Fig. 4a–c

	Elementary diffusion processes (EDP)	$V_{16}H_9$	$V_{15}MoH_9$	$V_{15}CrH_9$
Exp. [15, 16]	Unknown	0.266	0.240	0.289
Calculated activation energy via O sites	c–$C1$–1	0.837	0.997	0.706
	c–$C2$–2	0.452	0.658	0.399
	2a–$Z2$–2a	0.227	0.230	0.139
Calculated activation energy via T sites	2b–d	0.264	0.253	0.276
	2a–2b	0.044	0.097	0.045
	2a–2	0.286	0.228	0.276
	2a–c	0.192	0.186	0.176

The ZPE corrections are included. The experimental data taken from Ref. [15, 16] are presented for comparison purposes

lowest among three proposed diffusion paths. In general, the activation energy of hydrogen diffusion between two nearest neighboring T sites was found to be lower than those via the O sites. Mo/Cr substitution strongly affects the energy barriers of the hydrogen diffusion via the O sites. Cr substitution can reduce the barrier, whereas Mo substitution can increase the barrier. Such effects cannot be recognized for the diffusion processes between two nearest neighboring T sites without crossing any O site. In detail, the results for three different diffusion pathways in Fig. 4a–c showed that both substitutional Mo and Cr into vanadium hydride slightly decreased the activation energies of hydrogen diffusion between T_{2a}–T_2, and T_{2a}–T_c. The activation energies of hydrogen migration between second-neighbor sites (via O sites) in vanadium hydride are high; the barriers vary on the order of 0.452–0.837 eV. Substitutional Mo or Cr atom changes the mobility of hydrogen to be higher or lower activation energy as 0.997 eV and 0.399 eV, respectively, if the hydrogen diffuses crossing unoccupied O sites.

The activation energy of hydrogen diffusion between two T sites (T_{2a} and T_2) without crossing O site is 0.286 eV. On the other hand, this value does not change significantly by Mo/Cr substitution. Therefore, the energy barrier of hydrogen diffusion along this pathway (a) via O site is quite high as 0.452, and Cr substitution can reduce the barrier to 0.399 eV. As a result, the energy barrier between neighboring T sites from our calculations suggests that the hydrogen diffusion for T sites is dominant. The calculated energy barrier of 0.264 eV in $VH_{0.5625}$ is very close to those in $VH_{0.68}$ and $VH_{0.82}$, which were experimentally estimated at 0.267 eV and 0.280 eV. The activation energy depends on the hydrogen content in the β-phase vanadium hydride.

Finally, we find that the hydrogen diffusion between the first neighboring T sites is dominant for pure, substituted Mo and Cr vanadium hydrides. The present results suggest

that the activation energy of these hydrides would be estimated by hydrogen migration directly from *T* site to the nearest neighboring *T* site without crossing *O*-site vacancy. In addition, the impurities of Mo and Cr into the β-phase vanadium hydride can affect the diffusion barrier via the *O*-site transition state. The migration barriers are sensitive to the *O*-site occupancy. The energy barrier in the order of 0.706–0.997 eV is sufficiently high, resulting in a small diffusion coefficient at low temperatures. Therefore, in order to enhance the diffusion of H along pathways via *O* sites, the high-temperature condition should be addressed.

3 Conclusions

Understanding of the formation of vanadium hydrides and alloying hydrides is important in designing the potential hydrogen storage materials. We investigated the atomistic behavior of hydrogen and the effects of Mo or Cr substitution in β-phase vanadium monohydride by using first principles density functional methods. Substitution of Mo and Cr changes the detailed shapes of interstices and changes the site occupation of hydrogen in the monohydrides phase. Fundamental processes of the interstitial-assisted mechanisms are systematically figured out, and specific values of the site energies are obtained with zero-point energy (ZPE) corrections. Calculated lattice parameters of $V_{1-x}M_xH_{0.5625}$ hydrides follow the same order as the ^{1}H NMR measurements. The ground state for monohydride phase of $VH_{0.5}$ is expected to be a BCT structure with hydrogen atoms at O_{Z1} sites. Upon increasing the hydrogen concentration, the preferable site of additional hydrogen is the *T* site, the preferred site is determined by the structural effect. Substitutional Cr and Mo enhanced the hydrogen occupations in *O* sites. The atomic charge of H atom acquires from the interactions with the metal lattice is calculated using Barder charge analysis. The Barder charge of hydrogen at the *T* sites is more than that at the *O* sites; this could be an indication of the dominance of the *T*-site occupation at high hydrogen concentration. The calculated energy barrier for hydrogen migration is reported to be low as 0.264 eV for the *T*-site hydrogen diffusion in vanadium hydrides. This value is in very good agreement with our experimental measurement of 0.266 eV. The results reflect that the additional H prefers to migrate directly from *T* site to the nearest neighboring *T* site without crossing *O* site in both pure metal and alloy hydrides. Whereas the energy barrier in the order of 0.706–0.997 eV is sufficiently high for hydrogen diffusion via the *O* sites in these hydrides. Hence, in order to enhance the diffusion of H along pathways via *O* sites, the high-temperature condition should be addressed. The effects of the higher concentration of Cr/Mo substitution on hydrogen diffusion required further investigation to understand the enhancement of hydrogen diffusion by substitutional metals.

Acknowledgements The authors are thankful to the project on the establishment of Master's in Nanotechnology program of Vietnam Japan University for providing the facilities. This work was supported in part by a grant for research from Vietnam National University, Hanoi (VNU) under project number QG.15.09.

Compliance with ethical standards

Conflict of interest The authors declare that they have no conflict of interests.

References

1. Rosi NL, Eckert J, Eddaoudi M, Vodak DT, Kim J, O'Keeffe M, Yaghi OM (2003) Science 300:1127
2. Sakintunaa B, Darkrimb FL, Hirscherc M (2007) Int J Hydrogen Energy 32:1121
3. Schlapbach L, Züttel A (2001) Nature 414:353
4. Hauck J, Schenk HJ (1977) J. Less-Common Metals 51:251
5. Schober T, Wenzl H (1978) In: Alefeld G, Volkl J (eds) Hydrogen in metals II, topics in applied physics: application-oriented properties, vol 29. Springer, Berlin
6. Matsunaga T, Kon M, Washio K, Shinozawa T, Ishikiriyama M (2009) Int J Hydrogen Energy 34:1458
7. Fukai Y (2005) The metal-hydrogen system. Springer, Berlin
8. Akiba E, Iba H (1998) Intermetallics 6:461
9. Kubo K, Itoh H, Takahashi T, Ebisawa T, Kabutomori T, Nakamura Y, Akiba E (2003) J Alloys Compd 452:356
10. Shibuya M, Nakamura J, Enoki H, Akiba E (2009) J Alloys Compd 475:543–545
11. Tominaga Y, Nishimura S, Amemiya T, Fuda T, Tamura T, Kuriiwa T, Kamegawa A, Okada M (1999) Mater Trans, JIM 40(9):871
12. Kuriiwa T, Tamura T, Amemiya T, Fuda T, Kamegawa A, Takamura H, Okada M (1999) J Alloys Compd 433:293
13. Tamura T, Kamegawa A, Takamura H, Okada M (1862) Mater Trans 2001:42
14. Tamura T, Kazumi T, Kamegawa A, Takamura H, Okada M (2002) Mater Trans 42:2753
15. Asano K, Hayashi S, Nakamura Y, Akiba E (2010) J Alloys Compd 507:399
16. Asano K, Hayashi S, Nakamura Y, Akiba E (2012) J Alloys Compd 524:63
17. Johansson R, Ahuja R, Eriksson O, Hjorvarsson B, Scheicher RH (2015) Sci Rep 5:10301
18. Kim J, Yoo J-H, Cho S-W (2014) Mater Chem Phys 48:533
19. Schulz R, Boily S, Zaluski L, Zaluka A, Tessier P, Strom-Olsen JO (1995) Innov Metal Mater 63:529
20. Mananes A, Duque F, Mendez F, Lopez MJ, Alonso JA (2003) J Chem Phys 119:5128
21. Yarovskya I, Goldbergb A (2005) Mol Simul 31:475
22. Masuda J, Hashizume K, Otsuka T, Tanabe T, Hatano Y, Nakamura Y, Nagasaka T, Muroga T (2007) J Nucl Mater 1256:363
23. Hohenberg P, Kohn W (1964) Phys Rev 136:B864
24. Kohn W, Sham LJ (1965) Phys Rev 140:A1133
25. Kresse G, Hafner J (1993) Phys Rev B 47:558
26. Kresse G, Joubert D (1999) Phys Rev 59:1758
27. Kresse G, Hafner J (1994) Phys Rev B 49:14251
28. Kresse G, Furthmller J (1996) Comput Mater Sci 6:15
29. Vanderbilt D (1990) Phys Rev B 41:7892

30. Monkhorst HJ, Pack JD (1976) Phys Rev B 13:5188
31. Methfessel M, Paxton AT (1989) Phys Rev B 40:3616
32. Henkelman G, Uberuaga BP, Jonsson H (2000) J Chem Phys 113:9901
33. Henkelman G, Arnaldsson A, Jónsson H (2006) Comput Mater Sci 36:254
34. Sanville E, Kenny SD, Smith SD, Henkelman G (2007) J Comput Chem 28:899
35. Tang W, Sanville E, Henkelman G (2009) J Phys: Condens Matter 21:084204
36. Noda Y, Masumoto K, Koike S, Suzuki T, Sato S (1986) Acta Cryst B42:529
37. Kajitani T, Hirabayashi M (1985) Zeitschrift fur Physikalische Chemie Neue Folge, Bd 145:S27
38. Ogawa H (2013) J Alloys Compd 580:S131